AD-A138 024 LOW TEMPERATURE QUARTZ CRYSTAL OSCILLATOR FAST WARM-UP 1/1
SAW OSCILLATOR..(U) CENTRE NATIONAL DE LA RECHERCHE
SCIENTIFIQUE BESANCON (FRANCE.. J J GAGNEPAIN ET AL.
UNCLASSIFIED NOV 83 RADC-TR-83-242 AFOSR-81-0191 F/G 9/5 NL

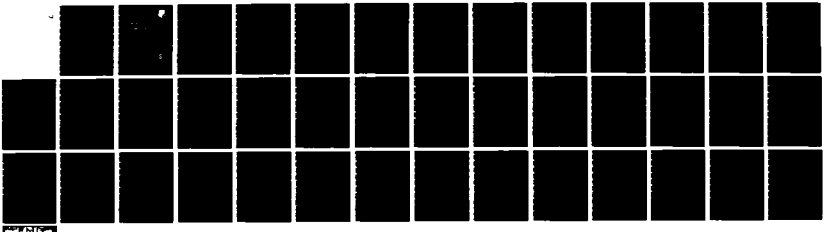

END
FILMED
4
DTIC

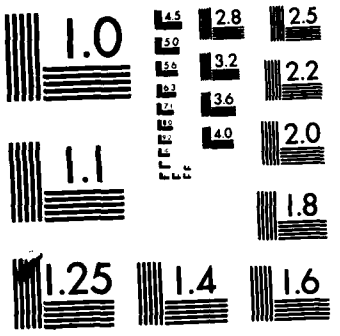

MICROCOPY RESOLUTION TEST CHART
NATIONAL BUREAU OF STANDARDS-1963-A

(12)

AD A138024

RADC-TR-83-242
Final Technical Report
November 1983

LOW TEMPERATURE QUARTZ CRYSTAL OSCILLATOR FAST WARM-UP SAW OSCILLATOR

Centre National de la Recherche Scientifique

Dr. J. J. Gagnepain and Dr. D. Hauden

APPROVED FOR PUBLIC RELEASE; DISTRIBUTION UNLIMITED

ROME AIR DEVELOPMENT CENTER
Air Force Systems Command
Griffiss Air Force Base, NY 13441

This report has been reviewed by the RADC Public Affairs Office (PA) and is releasable to the National Technical Information Service (NTIS). At NTIS it will be releasable to the general public, including foreign nations.

RADC-TR-83-242 has been reviewed and is approved for publication.

APPROVED: N. Yannoni

Nicholas Yannoni
Project Engineer

APPROVED: Harold Roth

HAROLD ROTH, Director
Solid State Sciences Division

FOR THE COMMANDER: Donald A Brantingham

DONALD A. BRANTINGHAM
Plans Office

If your address has changed or if you wish to be removed from the RADC mailing list, or if the addressee is no longer employed by your organization, please notify RADC (ESES) Hanscom AFB MA 01731. This will assist us in maintaining a current mailing list.

Do not return copies of this report unless contractual obligations or notices on a specific document requires that it be returned.

UNCLASSIFIED

SECURITY CLASSIFICATION OF THIS PAGE *(When Data Entered)*

REPORT DOCUMENTATION PAGE

READ INSTRUCTIONS BEFORE COMPLETING FORM

1. REPORT NUMBER: RADC-TR-83-242	2. GOVT ACCESSION NO.: AD A138024
3. RECIPIENT'S CATALOG NUMBER:	
4. TITLE *(and Subtitle)*: LOW TEMPERATURE QUARTZ CRYSTAL OSCILLATOR FAST WARM-UP SAW OSCILLATOR	5. TYPE OF REPORT & PERIOD COVERED: Final Technical Report 1 Jun 81 - 31 May 82
	6. PERFORMING ORG. REPORT NUMBER: N/A
7. AUTHOR(s): Dr. J. J. Gagnepain, Dr. D. Hauden	8. CONTRACT OR GRANT NUMBER(s): AFOSR-81-0191
9. PERFORMING ORGANIZATION NAME AND ADDRESS: Centre National de la Recherche Scientifique Laboratoire de Physique et Métrologie des Oscillateurs 32, av. de l'Observatoire 25000 Besancon France	10. PROGRAM ELEMENT, PROJECT, TASK AREA & WORK UNIT NUMBERS: 61102F 2305J133
11. CONTROLLING OFFICE NAME AND ADDRESS: Rome Air Development Center (ESES) Hanscom AFB MA 01731	12. REPORT DATE: November 1983
	13. NUMBER OF PAGES: 42
14. MONITORING AGENCY NAME & ADDRESS *(if different from Controlling Office)*: EOARD Old Marylebone Road London NW1 5TH U.K.	15. SECURITY CLASS. *(of this report)*: UNCLASSIFIED
	15a. DECLASSIFICATION/DOWNGRADING SCHEDULE: N/A

16. DISTRIBUTION STATEMENT *(of this Report)*

Approved for public release; distribution unlimited.

17. DISTRIBUTION STATEMENT *(of the abstract entered in Block 20, if different from Report)*

Same

18. SUPPLEMENTARY NOTES

RADC Project Engineer: Nicholas Yannoni (ESES)

19. KEY WORDS *(Continue on reverse side if necessary and identify by block number)*

Quartz	Low Temperature
Resonator	Surface Acoustic Wave (SAW)
Oscillator	Fast Warm-Up
Noise	Temperature

20. ABSTRACT *(Continue on reverse side if necessary and identify by block number)*

The objectives of this program are to:

- evaluate the frequency instabilities of quartz crystal resonators as a function of temperature and Q-factors,
- show the feasability of low temperature quartz oscillators,
- determine the dynamic thermal behavior of SAW quartz oscillators and the precise crystal orientation and wave propagation direction with minimized sensitivities.

DD FORM 1 JAN 73 1473 EDITION OF 1 NOV 65 IS OBSOLETE

UNCLASSIFIED

SECURITY CLASSIFICATION OF THIS PAGE *(When Data Entered)*

a) The contribution of impurities to finite Q-factor of quartz resonator at low temperature is studied, both theoretically and experimentally.

Short and long term frequency stability measurements are performed at low temperature with a dual crystal "passive" system adapted to liquid helium. Simultaneously temperature in the bath is controlled and correlation between frequency and temperature fluctuations is studied.

b) Dynamic temperature sensitivity of SAW oscillators is calculated by using a one-dimensional thermal model.

Crystal cut orientation and wave propagation direction are explored, at zero first order static temperature coefficient, in search of minimized dynamic thermal sensitivities.

A two-dimensional thermal diffusion model is achieved, for a later more realistic model.

LOW TEMPERATURE QUARTZ CRYSTAL OSCILLATOR

FAST WARM-UP SAW OSCILLATOR

Table of contents

A-1

CONTRIBUTIONS

Contributions of various portions of the program were made by the following staff members of L.P.M.O.

Mrs G. Théobald

MM. J. Groslambert

C. Paulin

G. Robichon

I - LOW TEMPERATURE QUARTZ CRYSTAL OSCILLATOR

GENERAL PRESENTATION

1/f noise remains the main limitation to the stability of quartz oscillators, when thermal noise and random noise are reduced. It has been demonstrated that 1/f noise level depends on the resonator Q-factor [1], following a $1/Q^4$ law.

Q-factor has a finite value on account of phonon interactions, but also because of impurity relaxation and diffusion. Therefore in this second part an analysis of impurity mechanisms was undertaken to determine their contribution to Q-factor and frequency fluctuations at low temperature.

Preliminary results on short and long term frequency stability of quartz resonators in liquid helium were obtained by using an adapted dual crystal passive system. The electronics was operated at room temperature and the crystal was in a copper can. Temperature was first controlled at 4K, and then near 1.5K in superfluid helium.

LOSS MECHANISMS DUE TO IMPURITIES

Superimposed on the phonon-phonon interaction losses, additional effects due to impurities can be observed at low temperatures. The common defects in quartz crystal are substitutional Al^{3+} atoms with charge compensating M^+ alkali ions. They are responsible for loss peaks, for instance at 50K for Na^+ ions. but also for a threshold in the loss-temperature characteristic for the lowest temperature.

1) Relaxation of interstitial alkali ions

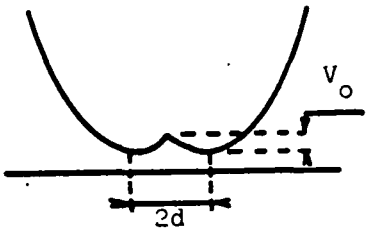

Fig. 1
Double-well potential

The most common interpretation of ionic conductivity in quartz crystals assumes that some Si^{4+} atoms are replaced by Al^{3+} associated with a monovalent alkali ion (Na^+, Li^+ or K^+ ..) achieving change neutrality in the crystal[2]. The ion occupies an interstitial site and is trapped in a double well potential (Fig. 1). It can jump from one position to the other one by thermal activation and cross over the potential barrier V_o.

The impurity is characterized by two quantum states with energy levels E_1, E_2 and energy splitting $E = E_1 - E_2$. If ω_{12}^o and ω_{21}^o are the probability densities of transition respectively from state 1 to 2 and 2 to 1, in the absence of sound wave, a relaxation time τ can be defined as

$$\frac{1}{\tau} = \omega_{12}^o + \omega_{21}^o \qquad (1)$$

If a sound wave is superimposed the energy spliting E is modulated by the corresponding high frequency strain η and takes the instantaneous value

$$E' = E + D\eta \qquad (2)$$

where D is the deformation potential.

Let n_o be the number of impurities per unit volume, and P_1 the probability of the impurity to be in state 1 with energy E_1 when in equilibrium.

$$P_1 = (e^{\beta E} + 1)^{-1} \qquad (3)$$

with $\beta = 1/k_B T$. T is the absolute temperature and k_B the Boltzmann constant.

The energy contribution of the impurities can be written [3]

$$E_t = n_o [P_1 (E + D\eta) + E_2] \qquad (4)$$

Differentiating with respect to strain gives the impurity contribution to the elastic stress.

$$\delta\sigma = \frac{n_o D^2 \eta}{1-i\omega\tau} \frac{\delta P_1}{\delta(E')} \tag{5}$$

where ω is the angular frequency of the sound wave.

This relation shows that when the impurity system is disturbed by the sound wave, a relaxation process occurs with time constant τ to restore equilibrium. There is a feedback of the change in population of impurity states to the elastic stress which leads for the sound wave to dispersion (feedback in phase) and to absorption (feedback out of phase).

The ratio $\delta\sigma/\eta$ gives the change δC of the elastic constant, from where is easily derived the velocity change δv and the attenuation α of the sound wave

$$\delta v = \frac{1}{2\rho v_o} \mathcal{R}_e \, (\delta C) \tag{6}$$

$$\alpha = - \frac{\omega}{2\rho v_o^3} I_m \, (\delta C) \tag{7}$$

ρ is the specific mass of the crystal and v_o the sound wave phase velocity.

From these two relations can be obtained the frequency shift and the Q-factor of the resonator

$$\frac{1}{Q} = \frac{n_o D^2}{4 \rho v_o^2 k_B T} \left(\frac{\omega_o \tau}{1 + \omega_o^2 \tau^2}\right) \tag{8}$$

$$\frac{\omega - \omega_o}{\omega_o} = - \frac{n_o D^2}{8 \rho v_o^2 k_B T} \left(\frac{1}{1 + \omega_o^2 \tau^2}\right) \tag{9}$$

The process which allows the impurity to cross over the potential barrier V_o of the double well potential is a thermal activation process. It can be easily shown that it is governed by an Arrhenius type law

$$\frac{1}{\tau} = 2\nu_o \, e^{- V_o / \langle E_o \rangle} \tag{10}$$

where ν_o is the jump frequency of the impurity, and $\langle E_o \rangle$ the mean energy of the harmonic oscillator composed of the impurity in one of the two quadratic potential wells.

If $k_B T >> h\nu_o$, then $\langle E_o \rangle \simeq k_B T$ and the relaxation time constant simply is

$$\frac{1}{\tau} = 2\nu_o \; e^{-V_o/k_B T} = \tau_o \; e^{-V_o/k_B T} \qquad (11)$$

ν_o corresponds to the eigenfrequency of the harmonic oscillator

$$\nu_o = \sqrt{\frac{V_o}{2m\, d^2\, \pi^2}} \qquad (12)$$

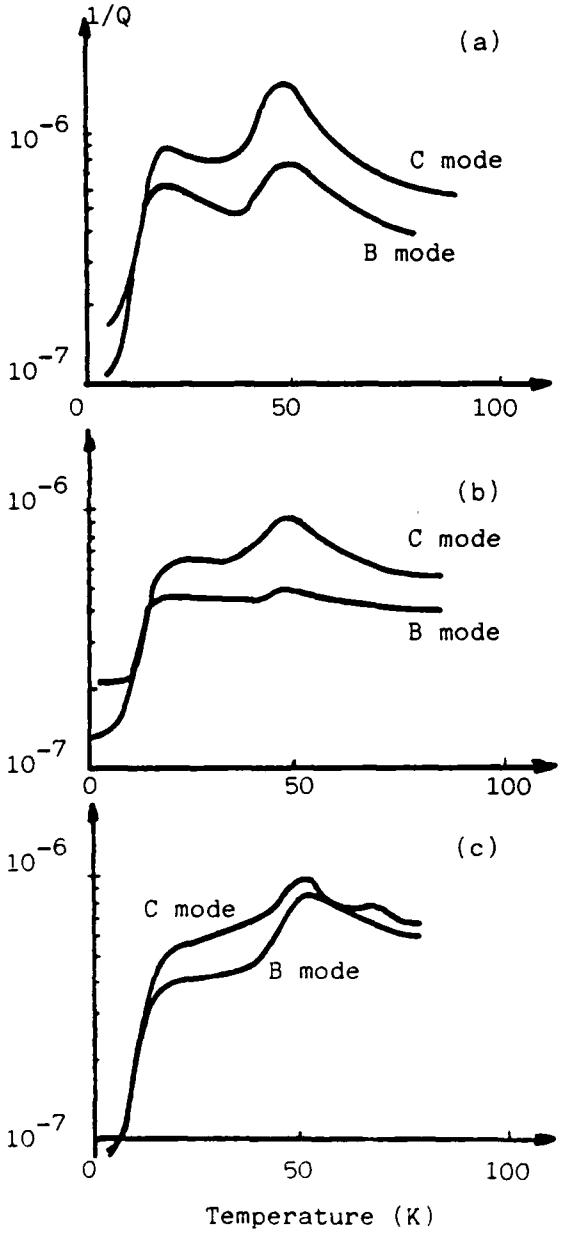

Fig. 2
Low temperature acoustic losses for the two shear modes
a) FC cut 246
b) FC cut 247
c) SC cut 206

The acoustic losses (1/Q) were measured on the B and C modes of SC and FC doubly rotated-cut resonators, as shown on fig. 2.

Two peaks can be observed. The 20K-peak is due to the crystal lattice anharmonicities and corresponds to interaction of one sound wave phonon with two thermal phonons [4]. The second peak at 50K is attributed to Na^+ impurities [5]. It can be observed that B mode exhibits a lower peak than C mode in all cases. For each resonator this shows how in the same crystal, with the same impurity content and the same propagation direction, the peak intensity is altered when changing the wave polarization i.e. the deformation potential D. This difference cannot be explained only by the ratio of velocities. The temperature T_m of the peak maximum remains constant as expected from the relation

$$k_B T_m = - \frac{V_o}{Ln\ (\omega_o \tau_o)} \qquad (13)$$

which does not depend on the deformation potential.

By substracting in the curves of Fig. 2 the background losses due to phonon interactions the contributions of impurity relaxation were obtained and are given on Fig. 3.

Adjusting parameters of relation 8 theoretical curves (dotted lines) were fitted to the experimental ones (continuous lines). This curve fitting enables one to evaluate the value of the relaxation time constant $\tau_o = 2.5.10^{-12}$ s, the potential barrier height $V_o = 0.040$eV and the distance between the two wells $2d \simeq 8$ Å.

These results show that the low temperature relaxation gives information on the Al^{3+}-M^+ defect structure. The impurity content n_o cannot be directly obtained from such measurements because the losses 1/Q depend on $n_o D^2$ where the deformation potential D is not known. However n_o could be determined by comparis with a reference crystal if its impurity concentration were known and if the cut and the vibration mode are the same.

If one considers that the relaxation time constant τ is fluctuating by $\delta\tau$, this will produce a fluctuation $\delta\omega$ of the resonance frequency. From relation (9)

$$\frac{\delta\omega}{\omega_o} = \frac{\Delta E}{E_o} \frac{\omega_o^2 \tau^2}{(1 + \omega_o^2 \tau^2)^2} \frac{\delta\tau}{\tau} \qquad (14)$$

with $E_o = \rho v_o^2$ and $\Delta E = \frac{n_o D^2}{4 k_B T}$

Using relation (8) in (14) gives

$$\frac{\delta\omega}{\omega_o} = \frac{E_o}{\Delta E Q^2} \frac{\delta\tau}{\tau} \qquad (15)$$

This will also exhibit a $1/Q^4$-law between frequency and relaxation time fluctuations in the power spectral densities. This was already pointed out, with the same form, in the case of fluctuations due to phonon interactions [1].

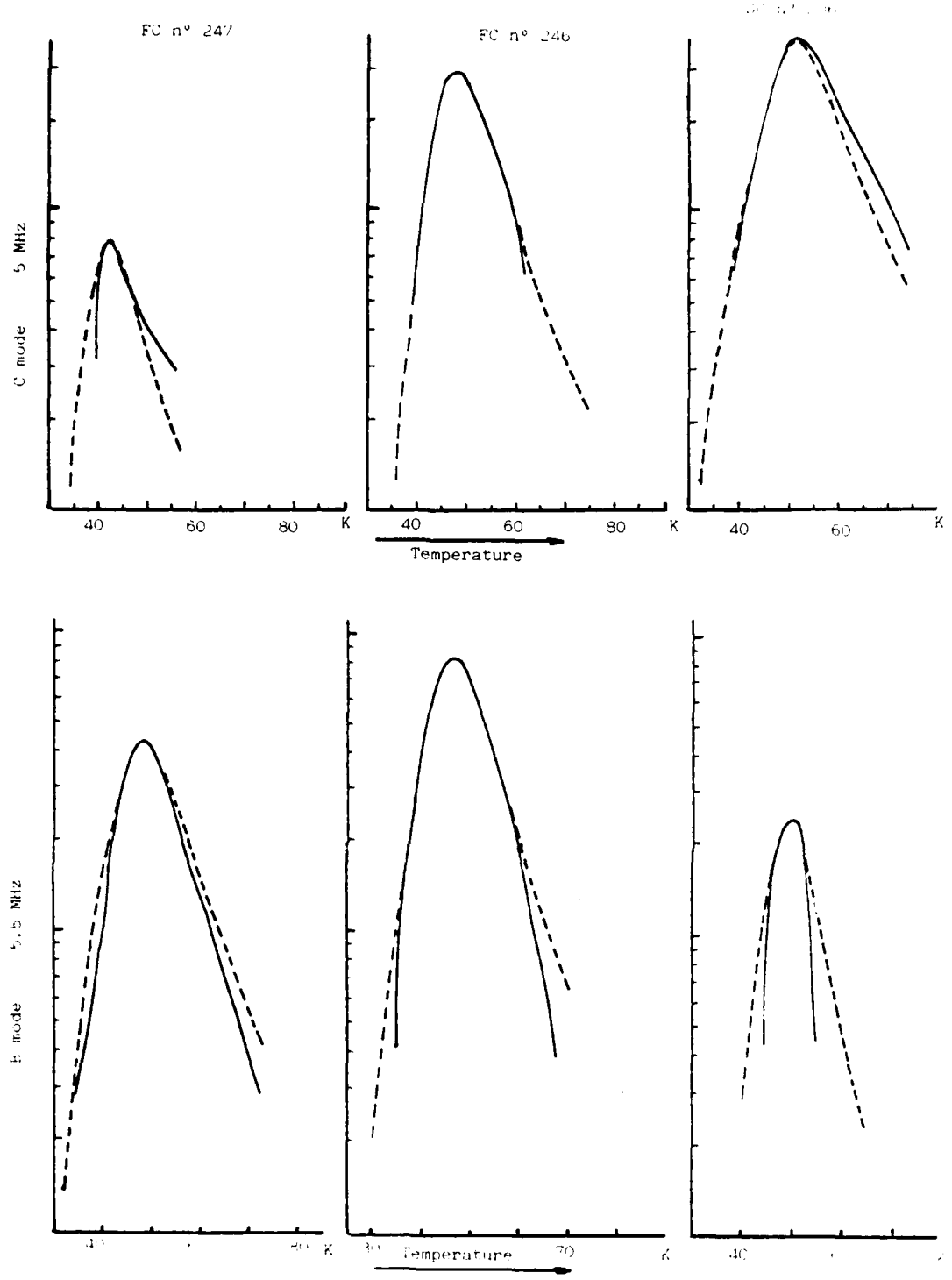

Fig. 3
Na^+ relaxation peaks in FC and SC-cut resonators

2) Sound wave phonon scattering by static defects

In addition to the previous relaxation of interstitial alkali ions is the scattering of the sound wave by the substitutional aluminium atoms replacing silicon. This can be considered as an isotropic effect which induces alteration of the kinetic energy by mass difference and of the potential energy by change of the linkages (equivalent to a change of some elastic constants). Both lead to similar absorption and only scattering by atoms of different mass will be considered here.

A linear chain of atoms with mass m has some substitutional atoms of mass $m+\Delta m$; the perturbed Hamiltonian can be written

$$W = W_o + \Delta W \tag{16}$$

where W_o corresponds to a perfect crystal and

$$\Delta W = \tfrac{1}{2}\, \Delta m\, (\partial u_n/\partial t)^2 \tag{17}$$

u_n is the displacement of an atom at the lattice site R_n

$$u_n = \frac{1}{\sqrt{Gm}} \sum_k \sqrt{\frac{\hbar}{2\omega_k}} \left[a_k\, e^{j\vec{k}.\vec{R}_n} + a_k^+\, e^{-j\vec{k}.\vec{R}_n}\right] \tag{18}$$

The sum is taken over all normal modes with wave number k and frequency ω_k. G is the number of atoms in the crystal. a_k and a_k^+ respectively are the annihilation and creation operators of the harmonic oscillator. Using (18) and (17) it can be shown that for n_o impurities per unit volume randomly distributed in the crystal

$$\Delta\omega = -\frac{n_o\, \Delta m\, \hbar}{4mG} \sum_{kk'} \sqrt{\omega_k \omega_{k'}}\, \left[a_k\, a_{k'}^+ + a_k^+\, a_{k'}\right] \tag{19}$$

Let N_k et $N_{k'}$ be the phonon numbers in normal modes k and k'. Applying Fermi's Golden Rule gives the transition probability and then the rate at which phonons are scattered from mode k.

$$\frac{dN_k}{dt} = \frac{n_o \pi}{8} \frac{\Delta m^2}{m^2 G^2} \sum_{k'} \omega_k\, \omega_{k'}\, \left[(N_k+1)N_{k'} - N_k(N_{k'}+1)\right]\, \delta(\omega_k - \omega_{k'}) \tag{20}$$

δ is the Kronecker symbol and $\delta(\omega_{k'}-\omega_k)$ assumes conservation of energy. If considering that all modes k' are in thermal equilibrium, equation (20) can be easily solved [6]. However if interactions between thermal phonons are taken into account a system of first order linear differential equations must be considered as a whole.

Let $\overline{n_k}$ and $\overline{n_{k'}}$ be the phonon numbers when in thermal equilibrium

$$\overline{n_k} = [e^{\hbar\omega_k/k_BT} - 1]^{-1} \tag{21}$$

and

$$N_k = \overline{n_k} + n_k \tag{22}$$

$$N_{k'} = \overline{n_{k'}} + n_{k'} \tag{23}$$

The conservation of energy implies $\omega_k = \omega_{k'}$ and therefore $\overline{n_k} = \overline{n_{k'}}$. Thus the set of equations similar to (20) becomes

$$\frac{dn_k}{dt} = K \sum_{k'} (n_{k'} - n_k) \tag{24}$$

with $K = \frac{n_o \pi}{8G^2} \left(\frac{\Delta m}{m}\right)^2 \omega_o^2$ and $\omega_o = \omega_k = \omega_{k'}$

Time dependent solutions of the form $n_k = a_k e^{-t/\tau}$ can be used. This leads to the new time-independent system

$$a_k = K \tau \sum_{k'} (a_k - a_{k'}) \tag{25}$$

which has the eigenvalues

$$1/K\tau = \infty \tag{26}$$

and

$$\left[\frac{1}{K\tau} - (p + 1)\right]^p = 0 \tag{27}$$

p being the total number of possible values of k' at the frequency ω_k. The degenerated eigensolution is equivalent for large p to

$$1/K\tau \simeq p \tag{28}$$

The total number of k' values is obtained by integrating in the k-space over the surface $\omega_k = \omega_{k'} = \omega_o$ and taking into account the three acoustic branches

$$p \simeq \frac{L^3 \omega_o^2}{2 \pi^2 C_o^3} \tag{29}$$

where $3/C_o^3 = 2/C_t^3 + 1/C_\ell^3$. C_t and C_ℓ respectively are the transverse and longitudinal sound wave velocities and L^3 is the crystal volume.

Thus

$$\frac{1}{\tau} = \frac{3 n_o L^3}{G^2} \left(\frac{\Delta m}{m}\right)^2 \frac{\omega_o^4}{16\pi C_o^3} \tag{30}$$

Introducing the lattice parameter a, the resonator Q-factor is

$$\frac{1}{Q} = \frac{3 n_o a^3}{16\pi G} \left(\frac{\Delta m}{m}\right)^2 \frac{\omega_o^3}{C_o^3} \tag{31}$$

This shows that 1/Q is temperature independant and will give a threshold for the lowest temperature when phonon interactions and interstitial impurity relaxation are minimized. But this effect appears to be neglegible at low frequencies.

LOW TEMPERATURE DUAL CRYSTAL PASSIVE SYSTEM

To perform frequency stability measurements on a resonator at low temperature with the electronics at room temperature the most convenient system is the dual crystal system [7] because of the distance between the inner part of the dewar and the outside.

1) Description

In fig. 4 is shown a schematic diagram of the system adapted to low temperature measurements.

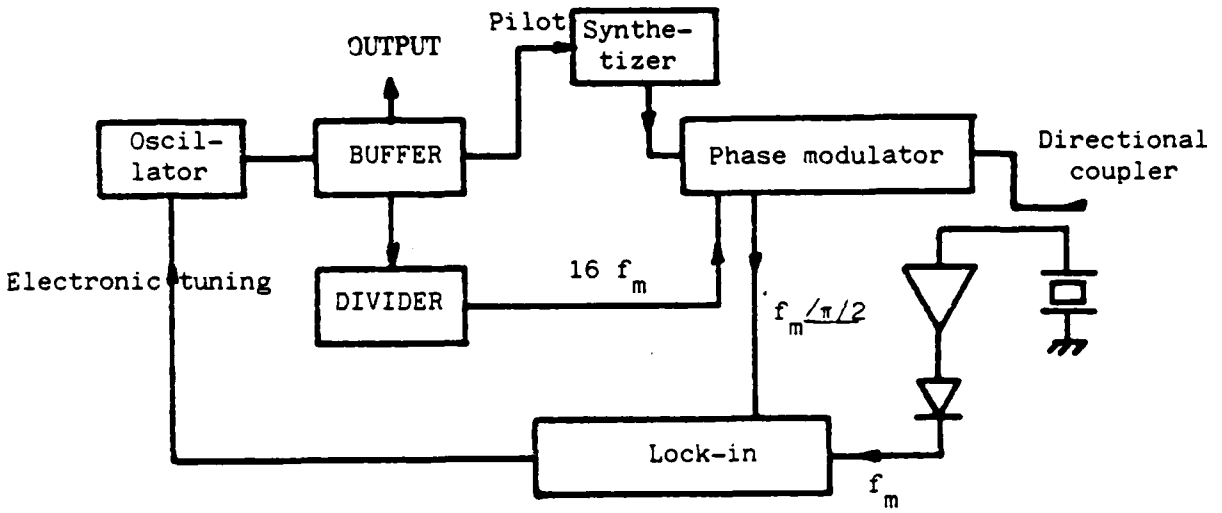

Fig. 4
Schematic diagram of dual crystal passive system

The output signal of the auxiliary quartz oscillator is phase modulated at a fixed frequency and then is passed through a directional coupler to the quartz resonator under test.

The reflected signal by the quartz is amplified and then detected. The auxiliary quartz oscillator is locked on the resonance frequency of the quartz inside the dewar with the help of a lock-in amplifier which is operated at the modulating frequency f_m.

The heart of this apparatus is the phase modulator which must be designed with care. As a matter of fact, the spurious amplitude modulation generated at the same time as the phase modulation, must be minimized, because this phase modulation after reflection on the quartz gives the amplitude modulation the modulation index of which is proportional to the difference frequency between the auxiliary oscillator and the quartz. The set constituted by the directional coupler and the reference quartz resonator works like a discriminator.

It appears that a modulation index of 10^{-5} (which gives an amplitude of -100 dB with regard to the carrier) produces a relative frequency shift of 10^{-13}. The phase modulation is an original design and is entirely digital.

The phase modulator

The phase modulation is obtained by using the time delay produced by a logic gate (Fig. 5) between the output and the input signals. Let ΔT be this time delay. It corresponds to a phase shift $\Delta\phi = 2\pi\ \Delta T/T$ where T is the period of the HF signal. By using n gates, it is possible to obtain a phase shift between 0 to $n\Delta\phi$ with n-steps.

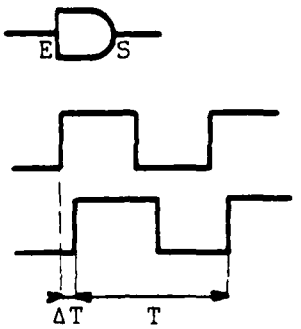

Fig. 5

A four bit multiplexer (Fig. 6) using eight gates leads to an output signal having a triangular phase modulation with a peak to peak phase shift of $2\pi/3$ (Fig. 7).

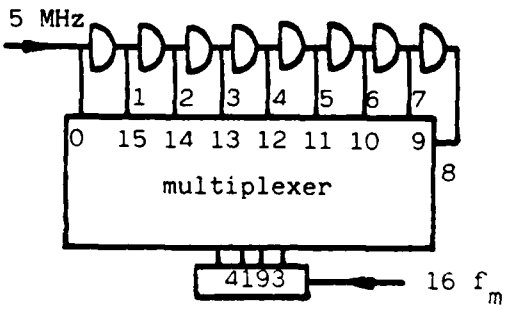

Fig. 6

This modulation waveform is obtained by connecting together the multiplexer inputs 1-15, 2-14, 3-13, 4-12, 5-11, 6-10, 7-9. The fundamental frequency modulation is equal to 1/16 of the driving frequency of the multiplexer states. This driving frequency is obtained by dividing the output signal of the auxiliary locked oscillator.

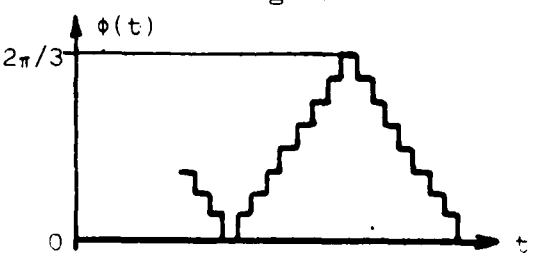

Fig. 7

In Fig. 8 are respectively represented the input signal (a), the output signal of the first gate with a phase shift of ΔT_o (b), the output signal of the second gate with a shift of $2\Delta T_o$ (c) the command signal (d) and the phase modulated output signal (e).

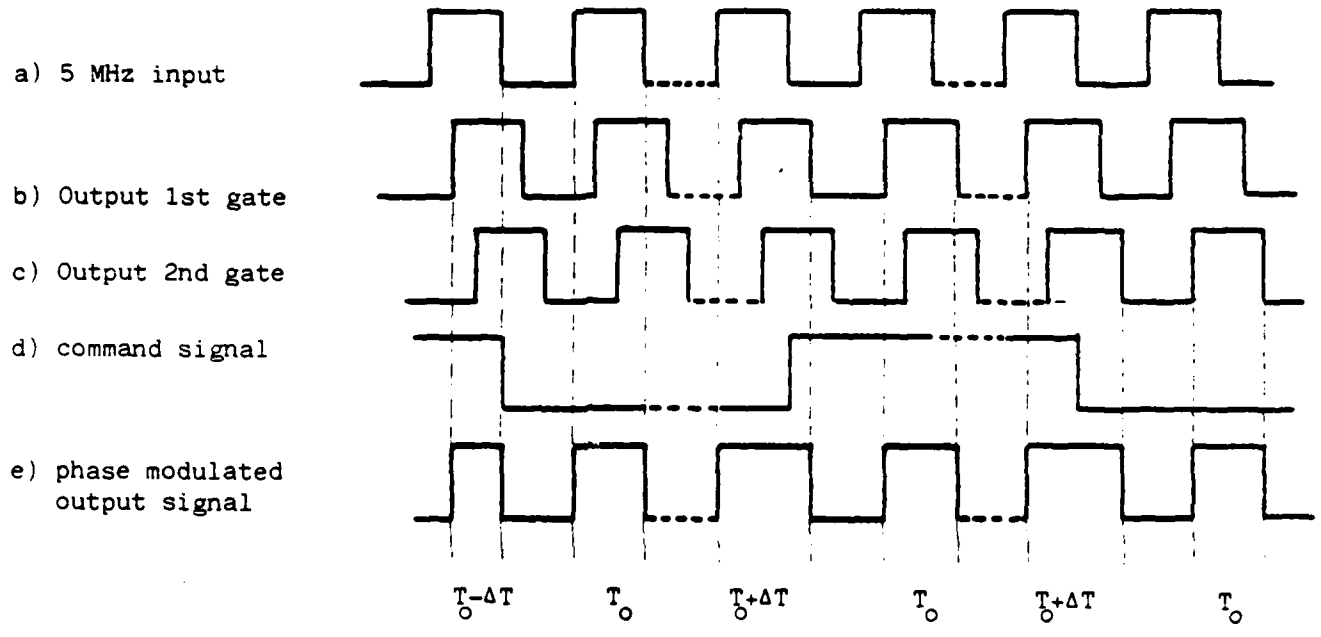

Fig. 8

The last pulse width at the commutation time is not equal to T_o where T_o is the ½ period of the 5 MHz signal. In fact, when the phase jump is positive (for the 0 to 8 multiplexer states) the pulse width increases by ΔT and when the phase jump is negative (for the 8 to 15 multiplexer states) the pulse width decreases by ΔT. In Fig. 9, we show the pulse width versus time, we obtain eight pulses larger and eight pulses smaller than the mean T_o. Since the pulse amplitude is constant the index modulation can be expressed by

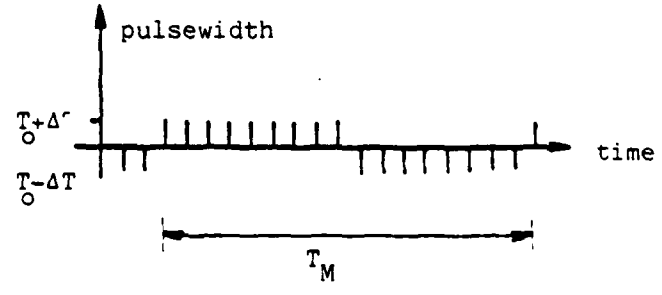

Fig. 9

$$\frac{8\ \Delta T}{T_o \times \text{number of pulse on a half period of modulation}}$$

For a 400 Hz frequency modulation with a ΔT of 8 ns and a fundamental frequency of 5 MHz, this modulation "index" is equal to 6×10^{-5} (or -83 dB).

In fact experiments give -60 dB ; this difference is due to the overshoot when the commutation occurs.

The amplitude modulation rejection factor can be increased by using a monostable which gives a constant pulse width. Thus the amplitude modulation can be rejected to -100 dB.

Buffer

This "cascade" buffer gives the possibility of obtaining three outputs from one input with a feedback coupling of 100 dB. Each output feeds respectively the phase modulator, the divider, which gives the modulation frequency and the third output which gives the 5 MHz signal.

Directional coupler

The coupling factor of the directional coupler is 10 dB. This is a commercial one. Its directivity is 40 dB. A better directivity would be desirable but is not available.

Amplifier - Detector

It permits on the one hand amplification of the signal reflected by the quartz to a level sufficient to be detected by a diode and on the other hand presentation of a constant load to the output of the directional coupler, which is the load as seen by the resonator under test.

Lock-in amplifier

This lock-in amplifier consists of two amplifiers with respective phases which are out-of-phase. The outputs of the amplifiers are sampled at the half period of the modulation frequency and then summed on a resistor.

The sampling signal is always in quadrature with respect to the excitation signal for all the modulation frequencies.

Synthesizer

The resonance frequency of the quartz at low temperature presents a shift of 5 KHz with respect to its value at room temperature. Therefore the auxiliary oscillator cannot be a Xtal oscillator, and a synthesizer must be used in the loop. This enables one to obtain a 5 MHz output frequency whatever the frequency of the resonator is in a 4 to 6 MHz range.

Frequency measurements system

This system is essentially constituted by two frequency difference multipliers (FDM) which enhance the frequency fluctuations by a factor of 2×10^5. The schematic diagram of this system is given on Fig. 10.

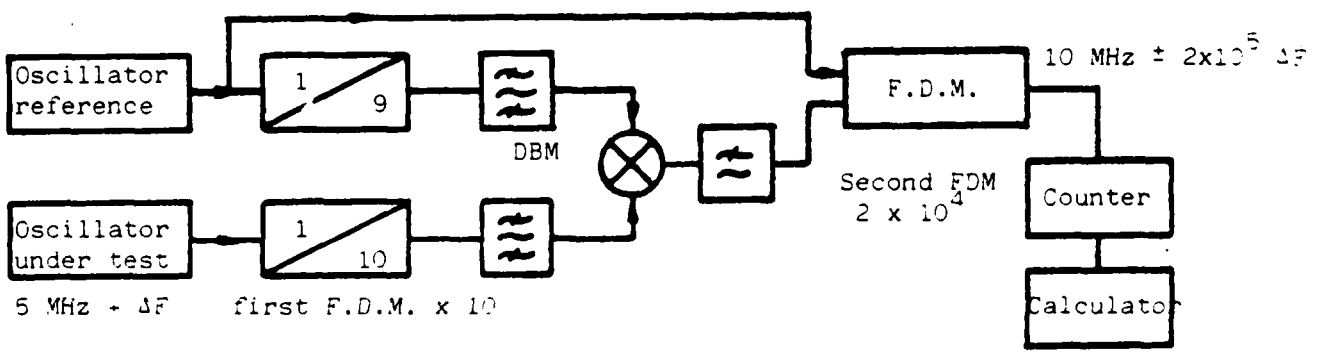

Fig. 10

The first FDM was built by the LPMO. Selective filters are inserted at the output of the frequency multipliers (x9 reference channel and x10 oscillator under test channel) in order to prevent the beat of the side bands of the two channel signals in the mixer. Just a selective filter after the mixer does not avoid these spurious signals, because they are at a frequency near the 5 MHz ± 10 Δf desired frequency.

The second FDM is a commercial unit which enhances by a factor of 2×10^4 the the difference frequency of the two signals connected at its inputs.

The measurement system noise versus integration time τ is given by fig. 11.

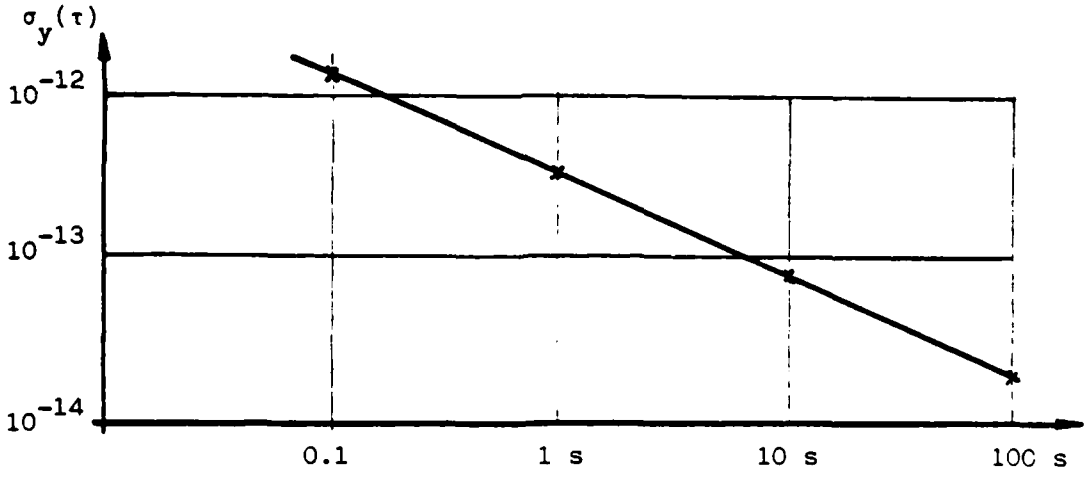

Fig. 11

2) Measurements

- temperature stability

Temperature control of the crystal in the helium dewar was performed by operating the crystal in a copper can sunk in the helium bath. Temperature was measured by means of a germanium resistor in an AC resistor bridge, resistance changes being detected with a lock-in amplifier. Temperature fluctuations were recorded at 4 K and at 1.5 K. The corresponding stability curves are presented in Fig. 12.

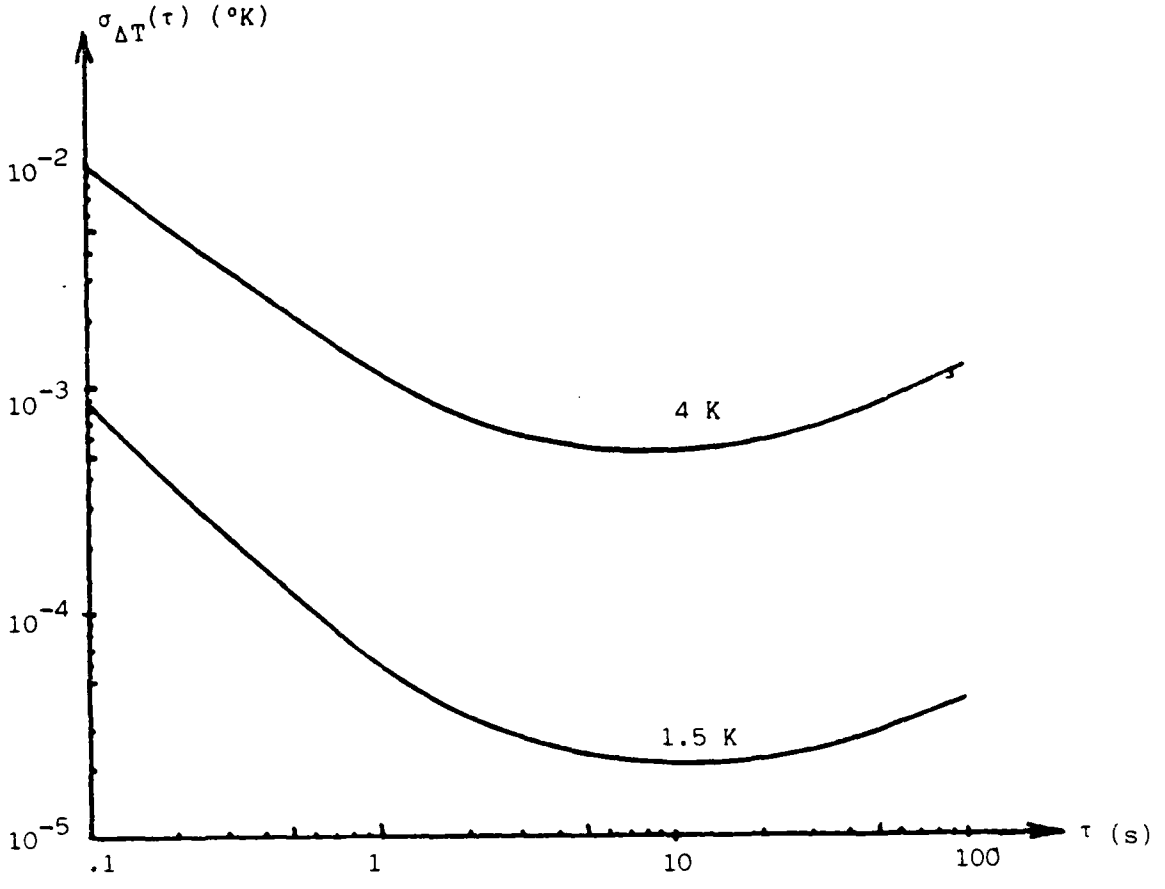

Fig. 12

Temperature stability at 1.5K and 4K

- Frequency stability

The frequency-temperature characteristics of quartz resonators at low temperature were measured between 4 K and 1.5 K and are given, for two resonators, in Fig. 13.

AT-cuts exhibits a general behavior corresponding to the lower curve, where the frequency temperature coefficient goes to zero with temperature.

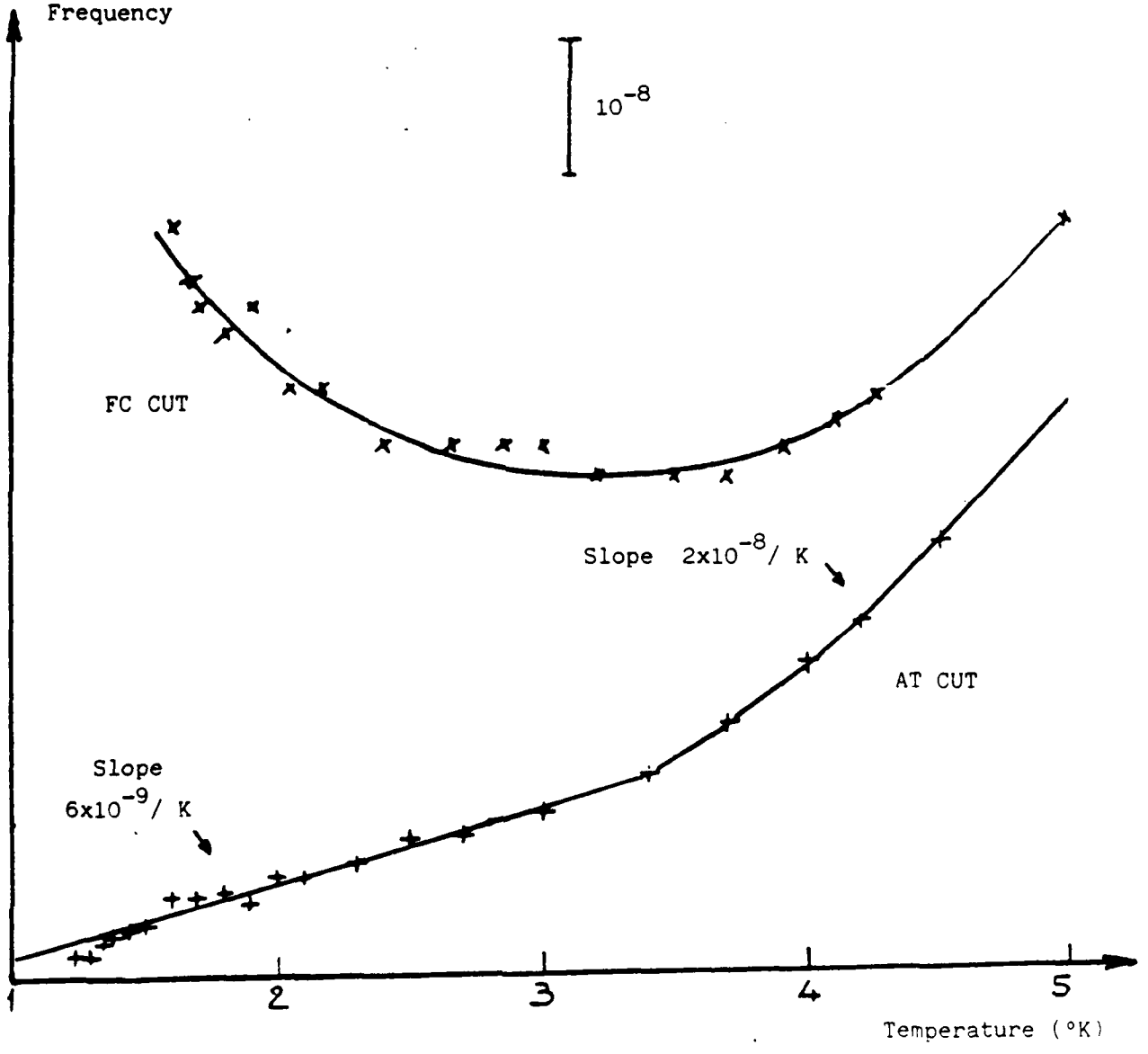

Fig. 13
Frequency vs temperature for FC and AT cut

This is what can be expected from the theory. At 1.5 K the temperature coefficient is of the order of 6.10^{-9}/°K. This gives an indication of the temperature stability which is necessary; for instance $1.6.10^{-5}$ K to achieve frequency stability of 1.10^{-13}. These numbers are to be considered only for the static thermal behavior of the crystal. The dynamic temperature coefficient of quartz resonators has not been evaluated, but would need to be considered in addition.

In the present state of the research, short term and long term frequency stability measurements were not yet performed with temperature controls operated at the same time.

Preliminary results were obtained with a resonator in the helium bath, but without temperature and pressure control. In this condition the result indicates a frequency stability of 4.10^{-12} for $10 < \tau < 100$ s at 4 K. These frequency fluctuations can be related to the temperature fluctuations of the free running bath which correspond to 2.10^{-4} K and at 4 K the frequency temperature coefficient of the crystal is 2.10^{-8}/°K.

CONCLUSION

Impurities can have two effects at low temperature : diffraction due to substitutional aluminum atoms and relaxation of interstitial alkalin ions. If the last one seems to have negligible influence, at least at low frequency, the first one can induce important relaxation peaks and lead to frequency fluctuations following the $1/Q^4$ law previously pointed out in the case of phonon-phonon interactions. Experimental verification will be the task of the next part of the project.

Electronics for operating quartz resonators at low temperature and for controlling temperature fluctuations were developed during the present period of the project.

Temperature stability of 2.5 10^{-5} K was obtained at 1.5 K. Taking into account the frequency temperature coefficient of the crystal, 6 10^{-9} K, this would correspond to a frequency stability of 1.5 10^{-13}. Measuring short and long term frequency stabilities will be the purpose of the next part of this study.

REFERENCES

(1) Low temperature quartz crystal oscillator, fast warm-up SAW oscillator. J.J. Gagnepain, D. Hauden. RADC-TR-81-184, Final report, July 1981.

(2) Dielectric losses of various monocrystals of quartz at very low temperatures. J. Volger, J.M. Stevels, C. van Amerongen. Philips Res. Rep. 10, 260 (1955).

(3) Elastic effects of structural relaxation in glasses at low temperatures. J. Jäckle et al. J. Non Crystalline Solids, 20 (1976).

(4) Interaction of sound waves with thermal phonons in dielectric crystals. H.J. Maris, Physical Acoustics, vol. VIII, Academic Press (1971).

(5) Impurities and anelasticity in crystalline quartz. D.B. Fraser. Physical Acoustics, vol. V, Academic Press (1968).

(6) The scattering of low-frequency lattice waves by static imperfections. P.G. Klemens, Proc. Phys. Soc., A 68, 1113 (1955).

(7) A systems approach to high performance oscillators. S.R. Stein et al. Proc. 32nd An. Freq. Cont. Symp., USAERADCOM, Ft Monmouth, N.J. (1978).

II - FAST WARM-UP SAW OSCILLATOR

GENERAL PRESENTATION

Generally, thermal behavior of SAW oscillators is due at the same time to slow temperature variations (temperature drifts) and fast temperature variations (temperature instabilities of thermostats or thermal transients of warm-up oscillators).

In the present work, only fast temperature variations are to be considered. In this case, a spatial distribution of temperature within the crystal arises. Thermal effects involve temperature gradients which induce stress and strain distribution. This is the "Dynamic thermal behavior" [1]-[2]. Thermal stresses and strains are coupled with the high frequency surface acoustic wave by crystal nonlinearities. Therefore velocity and frequency are shifted.

In a previous interim report (July 1981), a one-dimensional model of temperature distribution was presented. The perturbation method used to calculate corresponding frequency shifts led to numerical results. Comparison with experimental data showed some differences. Consequently a new model of temperature distribution is required in order to explain the dynamic thermal behavior.

The present work shows that :

- the measured dynamic temperature coefficient $\tilde{a}$ is small for quartz cuts having zero first order static temperature coefficients.
- experimental values of $\tilde{a}$ for ST-cut and FST-cut are $5.6\ 10^{-6}$ s/K and $(-1.0 - 3.0)10^{-6}$ s/K respectively.
- theoretical results obtained by using a new one-dimensional thermal model are in good agreement with the experimental results.

The theoretical study is developed along the following lines :

- calculation of temperature distribution in a one-dimensional model taking into account fast thermal exchanges between the crystal plate and the surrounding medium.
- calculation of corresponding stresses and strains leading to the theoretical values of dynamic temperature coefficient $\tilde{a}$ by using a perturbation method.
- to take into account the mechanical mounting of the quartz-plate, a two-dimensional model of temperature diffusion is developed.

ONE-DIMENSIONAL MODEL

A one-dimensional model has been used. It consists of a crystal plate of 2h-thickness and of infinite length along Oy and Oz.

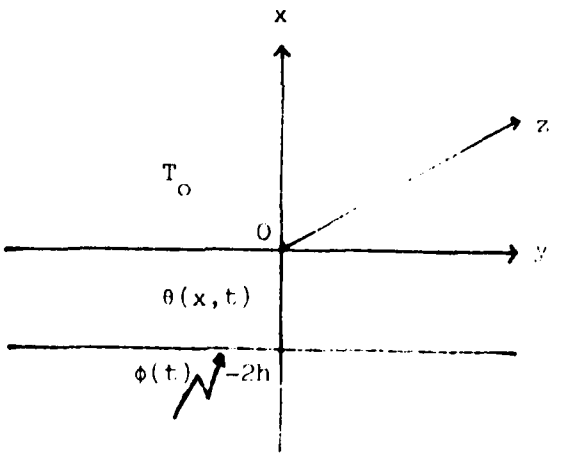

Fig. 1

One-dimensional temperature distribution

The bottom of the plate is submitted to temperature variation $\phi(t)$. Heat exchanges with the surrounding medium at temperature T_o occur on the upper surface of the device. This heat transfer is considered to be linear and characterized by the transfer coefficient H.

Let $\theta(x,t)$ be the temperature inside the crystal. The boundary-conditions are the following

$$\theta\ (-2h,\ t) = \phi(t) \tag{1}$$

$$\frac{d\theta}{dx} + H\ (\theta - T_o) = 0 \qquad x = 0 \tag{2}$$

Consequently temperature distribution within the crystal takes the form derived from the Duhamel theorem [3].

$$\theta(x,t) = \sum_{n=1} \frac{2\ (\beta_n^2 + 4h^2H^2)}{(2hH + 4h^2H^2 + \beta_n^2)} \sin \frac{\beta_n}{2h}\ (x+2h)\ \frac{\beta_n \kappa}{4h^2} \exp - \frac{\beta_n^2 \kappa t}{4h^2}\ I(t) \tag{3}$$

with

$$I(t) = \int_o^t \exp + \frac{\beta_n^2 \kappa t}{4h^2}\ \phi(\lambda)\ d\lambda \tag{4}$$

κ is the thermal diffusivity constant of the crystal in the x direction and β_n is the nth root of the transcendental equation

$$\beta \cot \beta + 2h\ H = 0 \tag{5}$$

Considering that $\phi(t)$ is a slowly varying function of time, the integration of $I(t)$ has been performed by parts and time derivatives higher than the first order are neglected. Then the temperature distribution is given by the relation

$$\theta\ (x,t) = \sum_{n=1} \frac{2\ (\beta_n^2 + 4h^2H^2)}{\beta_n\ (2hH + 4h^2H^2 + \beta_n^2)} \sin \frac{\beta_n}{2h}\ (x+2h)\ \left[\phi(t) - \frac{\dot{\phi}(t)}{\kappa\ \beta_n^2/4h^2}\right] \tag{6}$$

$\dot{\phi}(t)$ is the first time derivative of $\phi(t)$.

Since the internal temperature $\theta(x,t)$ presents a spatial distribution, thermal stresses and strains appear.

Because of the small thickness of the plate with respect to the other dimensions, no tensions are supported in the thickness direction. Following Holland [4], the adiabatic deformations and stresses are evaluated by taking into account mechanical boundary conditions corresponding to a plate which is free to expand.

Frequency shifts are deduced from formulas for stresses, strains and deformations by the method presented in the previous 1981-report. As in this calculation, summation appearing in relation (6) is truncated after the sixth term.

$$\frac{\Delta\omega}{\omega_o} = a\,\Phi(t) + \tilde{a}\,\dot{\Phi}(t)$$

at reference temperature equal to zero.

If reference temperature T_o is different from zero, this relation is written in the following form:

$$\frac{\Delta\omega}{\omega} = a\,[\Phi(t) - T_o] + \tilde{a}\,\dot{\Phi}(t)$$

In the usual temperature range from 0°C to 100°C the value of $\tilde{a}$ is not dependent on the point of the frequency-temperature characteristic, because T.C.'s of elastic and piezoelectric constants have to be considered as constant in the first order.

Experimental results

Experiments on the dynamic thermal sensitivity were performed on different quartz cuts. SAW delay lines were submitted to temperature cyclings by using a temperature controlled oven [5].

Fig. 2 shows experimental curves obtained by sweeping temperature over a temperature range of 8°C about 10.5°C with sweep periods respectively equal to 885 s (a), 1 330 s (b) and 2 660 s (c) for a ST-cut quartz SAW delay line at frequency about 87.7 MHz.

The measured $\tilde{a}$ is equal to $5.6\ 10^{-6}$ s/K.

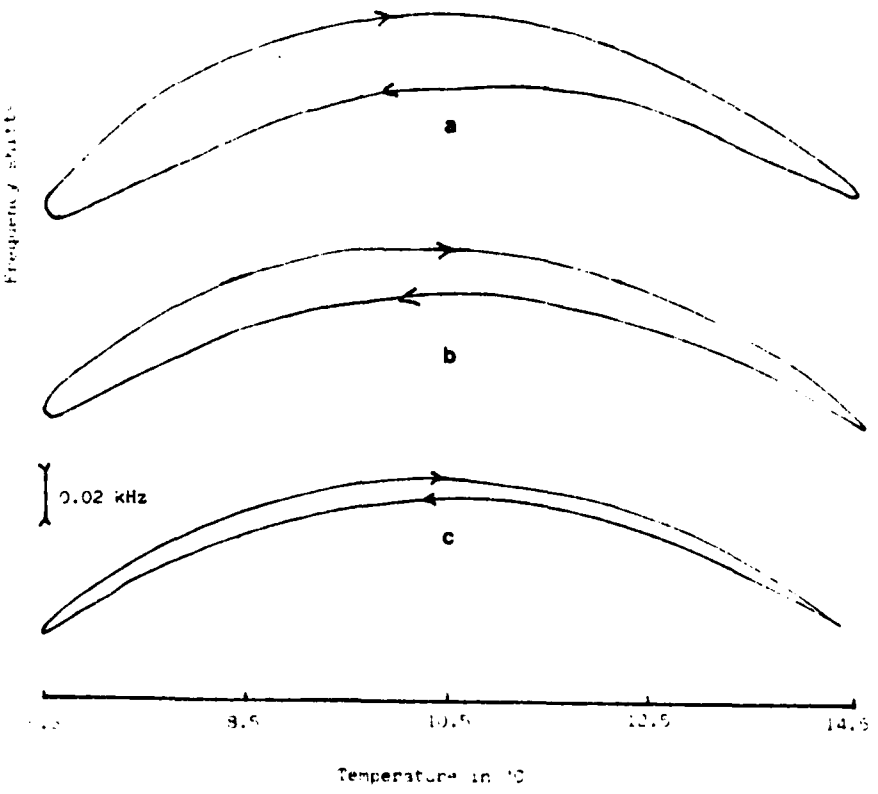

Fig. 2

Experimental sinusoïdal temperature cyclings

Table I summarizes measured values of $\tilde{a}$ for AT, ST and FST-cuts which have a turnover point of static frequency-temperature characteristics.

cuts	AT	ST	FST
$\tilde{a}$ measured (s/K)	$\sim 10^{-6}$	$5.6\ 10^{-6}$	$< 10^{-6}$

Table I
Values of the dynamic thermal coefficient $\tilde{a}$
for different orientations of quartz crystal

In temperature ranges beyond the turnover point, the presence of large frequency shifts coming from static temperature behavior (non-zero first order T.C.) makes it difficult to distinguish between static and dynamic effects and thus to reach the actual value of $\tilde{a}$. Consequently, it is interesting to get theoretical values of $\tilde{a}$ for quartz-cuts with zero first order static temperature coefficient.

Theoretical results

The dynamic coefficient $\tilde{a}$ was calculated for several cuts of quartz crystal as a function of the linear transfer coefficient H. To compare with the above-mentioned results, theoretical values of $\tilde{a}$ for ST and FST-cuts are reported in Table II, the normalized transfer coefficient 2hH being equal to 100. (see Appendix II)

cuts	ST	FST
$\tilde{a}$ theor. (s/K)	$-4\ 10^{-6}$	$0.13\ 10^{-6}$

Table II
One-dimensional theoretical values of $\tilde{a}$
for ST and FST cuts

Consequently, the one-dimensional theoretical model with linear transfer along the upper face of the plate seems to show that the FST cut has a smaller sensitivity to dynamic thermal effects than the ST-cut.

Because of the interest of studying cuts with zero first order static thermal coefficients, different double-rotation cuts (ϕ,θ,ψ) were studied and the theoretical $\tilde{a}$ calculated. The corresponding values are reported in Table III. ST and FST quartz are included for comparison as is the bulk SC cut.

Cuts	ϕ	θ	ψ	$\tilde{a}$ (s/K)	v (m/s)	Power Flow Angle
ST	0	42.5	0	$-4.0\ 10^{-6}$	3156	0
FST	6.34	-41.5	26	$1.3\ 10^{-7}$	3584	3.8
NEW CUTS	7	3.78	36	$-9.47\ 10^{-6}$	3271	2.7
	77	65.68	36	$-0.65\ 10^{-7}$	3317	-6.2
	77	67.4	27	$0.32\ 10^{-6}$	3395	-9.8
	80	17	27	$-0.5\ 10^{-6}$	3559	7.7
	102	11.06	45	$-0.12\ 10^{-6}$	3521	-1.4
BULK SC	22.5	34.3		$3.0\ 10^{-7}$	3608	

Table III
Theoretical values of $\tilde{a}$ for double rotation cuts with zero first order static thermal coefficient obtained with the one-dimensional model (angle values are in the standard YXw&t-notation)

It should be noted that any theoretical value $\tilde{a}$ is smaller than $1.0\ 10^{-6}$ s/K. Furthermore it is interesting to point out that the cut defined by angles ϕ = 77°, ϕ = 65.68° and ψ = 36° exhibits a T.C. $\tilde{a}$ weaker than $1.0\ 10^{-7}$ s/K. Also it seems reasonable to search for cuts with zero dynamic coefficient if at the same time, these cuts have a zero first order static temperature coefficient.

In order to model more completely the dynamic thermal behavior of SAW devices, a two-dimensional thermal diffusion model was built. In the axis system Oxyz the plate has an infinite length along Oz, and a cross section 2ℓ-long and 2h-thick (Fig. 3).

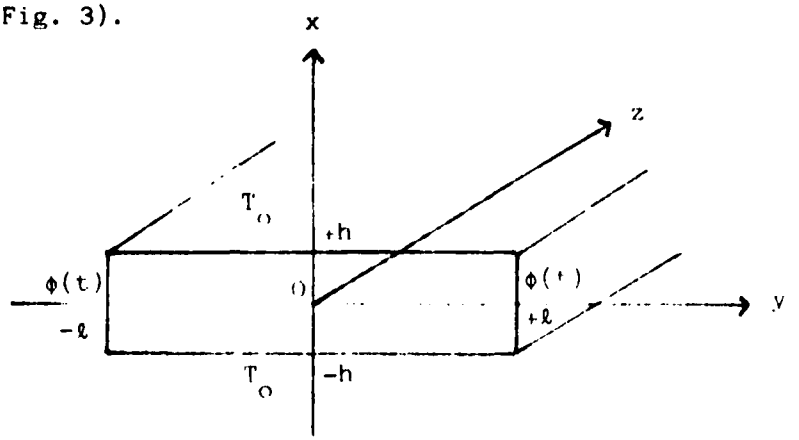

Fig. 3
Two-dimensional temperature distribution

A time variable temperature $\phi(t)$ is applied at $y = \pm \ell$. The boundaries $x = \pm h$ exchanges heat with the external medium maintained at T_o, with a linear heat transfer such

$$\frac{\partial \theta}{\partial x} + H (\theta - T_o) = 0 \qquad \text{at} \quad x = + h \tag{7}$$

$$- \frac{\partial \theta}{\partial x} + H (\theta - T_o) = 0 \qquad \text{at} \quad x = - h \tag{8}$$

The temperature (x,y,t) inside the plate obeys the diffusion equation

$$\frac{\partial^2 \theta}{\partial x^2} + \frac{\partial^2 \theta}{k^2 \, \partial^2 y} - \frac{1}{\kappa} \frac{\partial \theta}{\partial t} = 0 \tag{9}$$

where $k^2 = \lambda_x / \lambda_y$, λ_x and λ_y are the thermal conductivities along Ox and Oy and κ is the diffusion constant along Ox.

The boundary conditions are the following

$$\text{for } t > 0 \quad -h < x < h \qquad \begin{array}{lll} y = + \ell & \theta = \phi(t) \\ y = - \ell & \theta = \phi(t) \end{array} \tag{10}$$

and

$$\text{for } t > 0 \quad -\ell < y < \ell \qquad x = +h \qquad \frac{\partial \theta}{\partial x} + H(\theta - T_0) = 0$$
$$x = -h \qquad -\frac{\partial \theta}{\partial x} + H(\theta - T_0) = 0 \tag{11}$$

The initial conditions are

$$t = 0 \qquad \theta(x,y,0) = 0 \qquad -\ell < y < \ell \qquad -h < x < h \tag{12}$$

The solution of equation (9) with (10), (11), (12) is calculated in two steps

a) first, by calculating a peculiar solution, called $V(x,y,t)$ obtained with driving temperature $\phi(t)$ considered as a constant temperature ϕ.

b) then, the solution of the problem with a time dependant excitation $\phi(t)$ is obtained by application of the Duhamel theorem as in the one-dimensional model.

The first step (a) is solved along classical resolution methods of the diffusion equation with boundary conditions. Solutions are developed into series such as

$$V(x,y,t) = \frac{\sum_n 4H\phi \cos \alpha_n x}{[(\alpha_n^2 + H^2)h + H] \cos \alpha_n h} \frac{\cosh k\alpha_n y}{2\cosh k\alpha_n \ell} -$$
$$\sum_m (-1)^m \frac{(2m+1)}{4\ell^2 \left(k^2 \alpha_n^2 + \frac{(2m+1)^2\pi^2}{4\ell^2}\right)} \cos(2m+1)\frac{\pi y}{2\ell} e^{-k\left(\alpha_n^2 + \frac{(2m+1)^2\pi^2}{k^2 4\ell^2}\right)t} \tag{13}$$

α_n is the nth root of the transcendental equation

$$\alpha \tan \alpha h = H \tag{14}$$

Solution of the second step (b) corresponding to a variable $\phi(t)$ is given by the relation

$$v(x,y,t) = \sum_n \frac{4\,H\cos\alpha_n x}{n\left[(\alpha_n^2 + H^2)h + H\right]\cos\alpha_n h} \left[\frac{\phi(t)}{\cdots}\,\frac{\cosh k\alpha_n y}{\cosh k\alpha_n h}\right.$$

$$\left. - \sum_m (-1)^m \frac{(2m+1)\pi}{4}\,\frac{\kappa\,\dot{\phi}(t)}{(k\gamma_n^2)^2}\,\cdots\,\frac{\cdots}{\cdots}\right]$$

with $\gamma_n^2 = k^2\,\gamma_n^2 + \frac{(2m+1)^2\pi^2}{4\ell^2}$

This relation, like in the case of the one-dimensional model, has two terms. The first one is proportional to the applied temperature $\phi(t)$ and introduces frequency shifts as in static thermal behavior. The second one proportional to the first derivation of $\dot{\phi}(t)$ versus time is the term causing the dynamic thermal behavior.

CONCLUSION

Last experimental results indicate that SAW devices present a lower sensitivity to dynamic temperature effects than first experiments indicated. In particular a dynamic T.C. $\tilde{a}$ for ST-cut equal to 5.6 10^{-6} s/K and a smaller coefficient for FST-cut have been found.

A one-dimensional model taking into account a heat transfer function was used to reach theoretical values of the dynamic TC $\tilde{a}$ for several cuts having a zero first order static temperature coefficient. Values of $\tilde{a}$ are always smaller than 1.0 10^{-6} s/K. To model more accurately the dynamic thermal behavior of SAW oscillators, a two-dimensional model of thermal diffusion has been proposed.

In order to complete the above mentioned calculations the next steps in the work concerning a fast warm-up oscillator should be as follows:

- calculation of thermal stresses and strains in the two-dimensional model
- calculation of corresponding sensitivity in the case of cuts with zero first order static T.C. and comparison with previous results.

The information provided by this study may be used to find a quartz cut with dynamic thermal compensation as well as static temperature compensation.

REFERENCES

(1) G. Théobald, G. Marianneau, R. Prétot, J.J. Gagnepain, "Dynamic thermal behavior of quartz resonators", 33rd An. Freq. Cont. Symp., Fort Monmouth, 1979.

(2) A. Ballato and J. Vig, "Static and dynamic frequency-temperature behavior of signly and doubly rotated, oven controlled quartz resonators", Proc. 32nd An. Freq. Cont. Symp., Fort Monmouth, 1978.

(3) H. Carslaw and J. Jaeger, "Conduction of heat in solids", Oxford University Press, London, 1959.

(4) R. Holland, "Non uniformly heated anisotropic plates : II. Frequency transients in AT and BT quartz plates", Ultrasonics Symp. Proc., IEEE cat. 74 CHO 896-1SU (1974).

(5) D. Hauden, G. Théobald, "Dynamic thermal sensitivity of SAW quartz oscillators", IEEE Ultrasonics Symposium Proceedings, 1980.

APPENDIX I

Experimental temperature controlled oven for dynamic temperature effect measurements (fig. 4)

For this type of measurement, the device must have a very weak thermal inertia. We have chosen a temperature controlled oven with a flat heater. The SAW delay line is held on a face of the heater. Temperature measurements and control are performed with an H.P. temperature probe which is in contact with the heater on the other side.

2hH	ST	FST
100	$-4.0\ 10^{-6}$	$1.3\ 10^{-7}$
10	$-3.2\ 10^{-5}$	$1.5\ 10^{-6}$
1	$-2.6\ 10^{-4}$	$6.6\ 10^{-5}$
0.3	$-8.1\ 10^{-4}$	$5.5\ 10^{-4}$

$\hat{a}$ values for ST and FST cut
as a function of 2hH linear transfer coefficient

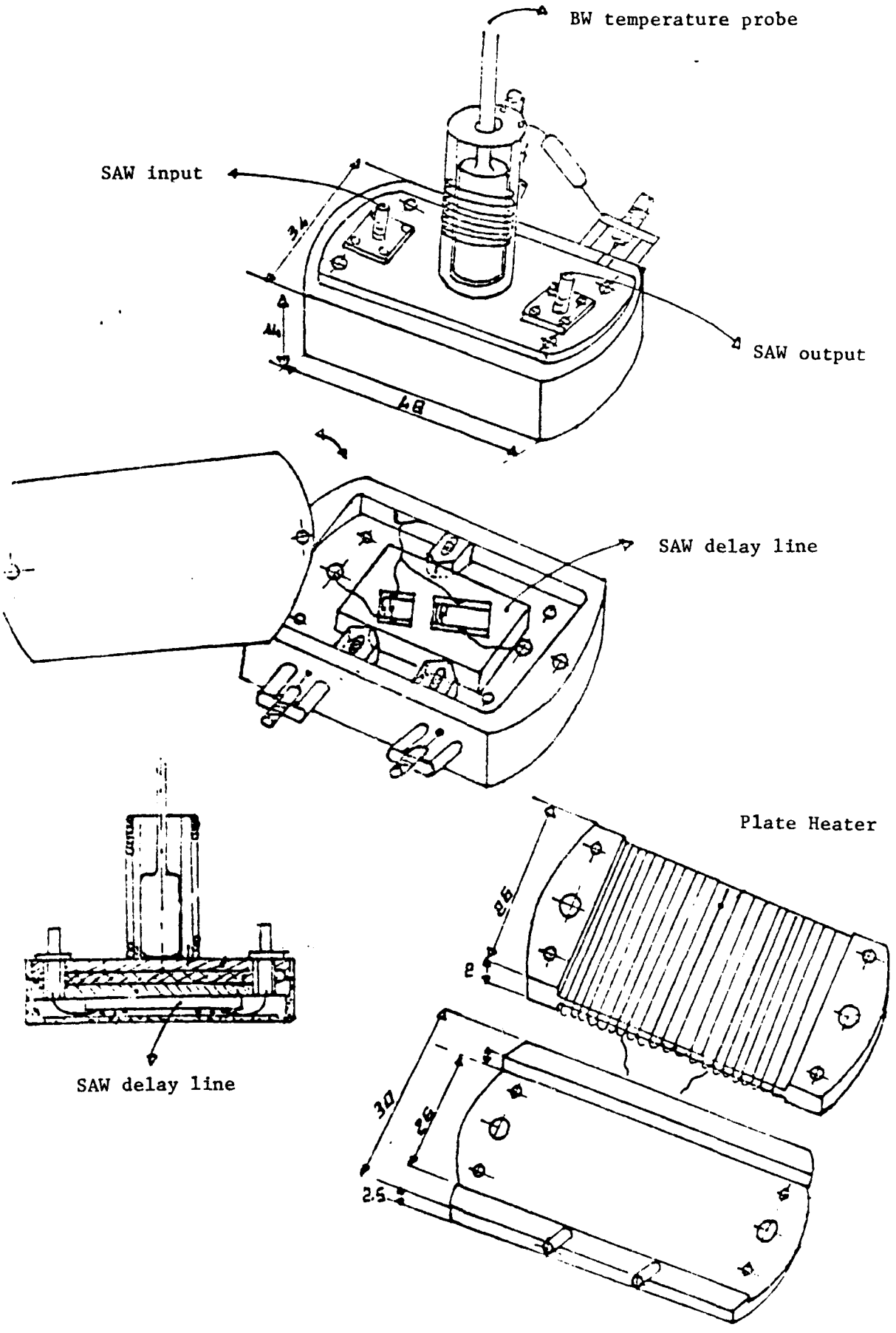
BW temperature probe
SAW input
SAW output
34
14
3
48
SAW delay line
SAW delay line
Plate Heater
26
2
30
25
2.5

Sizes in mm

MISSION
of
Rome Air Development Center

RADC plans and executes research, development, test and selected acquisition programs in support of Command, Control Communications and Intelligence (C^3I) activities. Technical and engineering support within areas of technical competence is provided to ESD Program Offices (POs) and other ESD elements. The principal technical mission areas are communications, electromagnetic guidance and control, surveillance of ground and aerospace objects, intelligence data collection and handling, information system technology, ionospheric propagation, solid state sciences, microwave physics and electronic reliability, maintainability and compatibility.

Printed by
United States Air Force
Hanscom AFB, Mass. 01731

END

FILMED

4-84

DTIC